# Modeling Nonparabolicity Effects in Silicon Inversion Layers

C. Troger, H. Kosina, and S. Selberherr
Institute for Microelectronics, TU Vienna
Gusshausstrasse 27–29, A-1040 Vienna, Austria
http://www.iue.tuwien.ac.at/

***Abstract*—We present a method to include the nonparabolicity correction for the bulk dispersion relation in the self-consistent solution of Schrö dinger and Poisson equation. A formalism has been derived which allows to characterize each subband by its energy, an effective mass and a subband nonparabolicity coefficient. A one-dimensional Schrödinger-Poisson solver has been developed which is applicable to both MOS and heterostructures. The program is applied to silicon inversion layers, and the influence of nonparabolicity on the subband system is quantitatively analyzed. As a consequence of nonparabolicity the wave functions depend on the in-plane momentum of the carriers.**

## I. Introduction

The inclusion of nonparabolic bands in the description of a quasi two-dimensional electron gas is a prerequisite for accurately modeling the electron transport at high driving fields. We present a numerical method to obtain a self consistent solution of Schrödinger's and Poisson's equations for a nonparabolic bulk band structure. The approaches presented in [2][3] solve the Schrödinger equation in real space representation, and require therefore some simplifications concerning the operator of the kinetic energy. We improved the technique described in [1] to include this operator without further simplifying assumptions. The result is a consistent treatment of nonparabolicity for the dispersion relation, the wave functions and the electron density. The developed formalism was implemented in a one-dimensional Schrödinger-Poisson solver which allows a very general specification of material parameters and geometrical structures.

## II. Formulation

### A. Schrödinger equation

A parabolic band structure is commonly assumed to describe a quasi two-dimensional electron gas. Owing to a strong confinement of the electrons near the $Si/SiO_2$ interface the quantization of electron states have to be treated by a system of discrete subbands.

We separate the three-dimensional wave function into a plane wave parallel to the interface $(x,y)$, describing the in-plane transport, and an envelope function in the normal direction $(z)$

$$\Psi(\mathbf{r}) = \psi(z) \exp\left(\imath \mathbf{K} \cdot \mathbf{r}_{\|}\right), \tag{1}$$

where $\mathbf{K}$ denotes the in-plane wave vector. Following the effective mass approach and including the nonparabolicity correction in the bulk dispersion relation

$$\mathcal{E}\left(1 + \alpha\mathcal{E}\right) = \frac{\hbar^2 K^2}{2m_{xy}} + \frac{\hbar^2 k_z^2}{2m_z}, \tag{2}$$

we have to solve the one-dimensional Schrödinger equation

$$\left(\hat{\mathbf{T}} + \hat{\mathbf{V}}\right)\psi(z) = E\,\psi(z) \tag{3}$$

In (3) $\hat{\mathbf{V}}$ denotes the operator describing the confining potential, and the operator of the kinetic energy can be formally written as

$$\hat{\mathbf{T}} = \frac{1}{2\alpha}\left(-1 + \sqrt{1 + 4\alpha\frac{\hbar^2}{2}\left(\frac{K^2}{m_{xy}} + \hat{\mathbf{G}}\right)}\right) \tag{4}$$

$$\hat{\mathbf{G}} = -\frac{\partial}{\partial z}\frac{1}{m_z}\frac{\partial}{\partial z}. \tag{5}$$

The form of operator (4) does not allow to separate the energy term $\hbar^2 K^2/2m_{xy}$ and will therefore introduce a dependence on the in-plane wave vector $K = (k_x, k_y)$ of both the eigenenergies and the wave functions. An analytical treatment of the operator (4) has to be performed in the eigenfunction space of the operator

$$\hat{\mathbf{G}}_{\|} = \frac{K^2}{m_{xy}} + \hat{\mathbf{G}}. \tag{6}$$

To avoid this, it has become common practice to solve the Schrödinger equation only for $\hat{\mathbf{T}} = \hbar^2/2\hat{\mathbf{G}}_{\|}$ and to treat the nonparabolic correction by means of a perturbation theory. For a silicon inversion layer we will neglect the penetration of the wave function in the oxide and can therefore choose a vanishing wave function as boundary condition. Thus the eigenfunctions $u_n$ of operator (5)

0-7803-3775-1/97/$10.00 

are sine functions. In fact, if the bulk nonparabolicity coefficient and the bulk masses do not depend on $z$, both $\hat{\mathbf{G}}_{||}$ and $\hat{\mathbf{G}}$ have the same set of eigenfunctions.

To solve the Schrödinger equation (3) we will use a method similar to the one described in [1]. In the base system consisting of a truncated set of eigenfunctions $u_n$ of the operator (6) the operator (4) can be written as a diagonal matrix.

As a consequence the spectral representation $\mathbf{a}$ of the envelope function $\psi(z)$ for a specific value of the magnitude $K$ of the in-plane wave vector is then obtained as the solution of the matrix eigenvalue problem

$$\left(\mathbf{T}_{(K)} + \mathbf{V}\right) \mathbf{a}_{(K)} = E_{n(K)}\, \mathbf{a}_{(K)}. \tag{7}$$

Note that because $\mathbf{T}$ depends on $K$ so do the the eigenvectors and eigenenergies. In particular, $E_n(K)$ represents the in-plane dispersion relation. In (7) T and V stand for matrices comprising the matrix elements of the operator for the kinetic and potential energy:

$$V_{n,m} = \int u_m(z) V(z) u_n(z) dz, \tag{8}$$

$$T_{n,m} = \frac{2\Gamma_n}{1+\sqrt{1+4\alpha\Gamma_n}} \cdot \delta_{n,m} \tag{9}$$

with $\Gamma_n$ denoting the eigenvalues of operator $\hat{\mathbf{G}}_{||}$, and $\delta_{n,m}$ as the Kronecker delta. The eigenenergies $E_n$ of (7) at different $K$-values are shown as points in Fig. 1.

### *B. In-plane dispersion relation*

After (7) the in-plane dispersion relation can be calculated point wise. However, it is desirable to obtain an analytic in-plane dispersion. In contrast to [2] [3] perturbation theory will only be used at this point to derive the $K$-dependence of the wave function and the eigenenergies for each subband analytically.

As stated below the deviation $\Delta\hat{\mathbf{T}}$ of the operator of the kinetic energy from its value at the subband minimum ($K = 0$) will be expressed in the eigenfunction space of the operator (6).

$$\Delta\hat{\mathbf{T}} = \sum_l \left(T_{1,l}K^2 + T_{2,l}K^4\right) \hat{\mathbf{P}}_l \tag{10}$$

$$T_{1,l} = \frac{\hbar^2}{2m_{xy}} \left(1+4\alpha\Gamma_l^0\right)^{-1/2}$$

$$T_{2,l} = -\alpha\frac{\hbar^4}{2m_{xy}^2} \left(1+4\alpha\Gamma_l^0\right)^{-3/2}$$

$\hat{\mathbf{P}}_n$ denotes the projection operator onto the eigenfunction $u_n$. Now we apply perturbation analysis where $\hat{\mathbf{T}}(K=0)$ represents the unperturbed problem, and $\Delta\hat{\mathbf{T}}$ is the perturbation operator. In this way, the in-plane dispersion relations $\mathcal{E}_n(k)$ are obtained as polynomials in $K^2$.

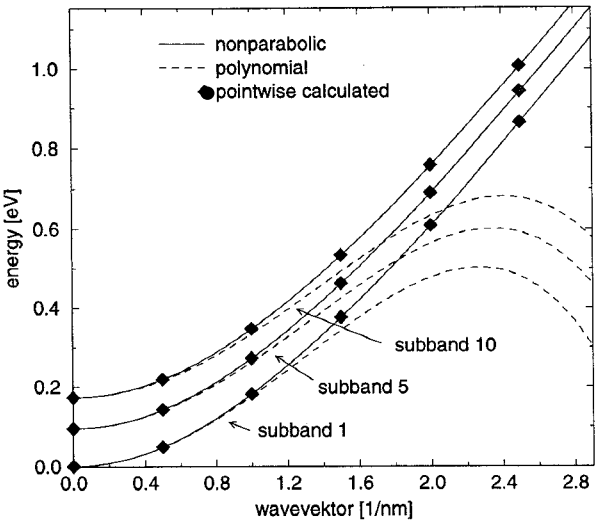


Fig. 1. Approximations for the energy to wave vector relation.

The dashed lines in Fig. 1 show the resulting polynomial for the first, fifth and tenth subband. We want to emphasize that this polynomial approximation is only valid for low energies, while it becomes even meaningless for larger wave vectors. Therefore, it seems favorable to assume nonparabolic dispersion relations after (11) instead of polynomials in $K$.

$$\left(\mathcal{E}_n - E_n^0\right)\left(1+\alpha_n(\mathcal{E}_n - E_n)\right) = \frac{\hbar^2 K^2}{2m_n}. \tag{11}$$

The effective subband mass, $m_n$, and the subband nonparabolicity coefficient, $\alpha_n$, are obtained by perturbation analysis.

$$m_n = \frac{\hbar^2}{2T_{1,nn}} \tag{12}$$

$$\alpha_n = -\frac{1}{T_{1,nn}^2}\left(T_{2,nn} + \sum_{m\neq n}\frac{|T_{1,mn}|^2}{E_n^0 - E_m^0}\right) \tag{13}$$

The matrix elements of the operator (10) have to be calculated with the subband wave functions at $K = 0$. Although perturbation theory was employed the above coefficients are exact since the neglected terms are $\mathcal{O}(K^6)$, while $m_n$ and $\alpha_n$ represent $\mathcal{E}_n(K)$ up to $K^4$.

### *C. Self-consistent iteration*

The electrostatic potential is computed in real space by using a finite difference discretization of Poisson's equation. This method only necessitates the solution of a tridiagonal linear equation system, which can be performed efficiently.

$$\frac{d}{dz}\epsilon\frac{d}{dz}\phi(z) = e\left(p(z) - n(z) + C(z)\right). \tag{14}$$

The potential energy needed in the Schrödinger equation is given by

$$V(z) = -e\phi(z) + E_C(z) \tag{15}$$

The net doping concentration $C(z)$ and the conduction band edge $E_C(z)$ have to be supplied on a grid, which needs to be uniform in the region where Schrödinger's equation is solved. For the hole density Boltzmann statistics and no quantization is assumed. To convert from momentum to real-space representation and vice verse the fast Fourier transform is employed. If $f$ denotes the Fermi-Dirac distribution function the electron density can be obtained by

$$n(z) = \sum_{K,n} |\psi_n(z,K)|^2 f(E_n(K)) \tag{16}$$

With the masses and the nonparabolicity coefficients defined in (11) and the valley degeneracy $g_v$, the density of states in each subband can be expressed as

$$\rho(\mathcal{E}_n - E_n^0) = \frac{g_v}{\pi\hbar^2} m_n \left(1 + 2\alpha_n(\mathcal{E}_n - E_n)\right). \tag{17}$$

This allows to transform the sum over all possible states into an integral over the energy:

$$n(z) = \sum_v \sum_n \int_0^\infty |\psi_n(z,K)|^2 f(\mathcal{E}_{\|} + E_n^0)\rho(\mathcal{E}_{\|}) d\mathcal{E}_{\|}. \tag{18}$$

To stabilize the self-consistent iteration the derivative $\mathrm{d}n/\mathrm{d}\phi$ has to be included in the linearized Poisson equation. An approximate derivative by using its value for the bulk case turned out to be sufficient.

$$\frac{\mathrm{d}n}{\mathrm{d}\phi} = \frac{n}{U_T} \frac{\mathcal{F}_{-1/2}(\eta)}{\mathcal{F}_{1/2}(\eta)} \tag{19}$$

$\mathcal{F}_{\pm 1/2}$ denote the Fermi integrals with the reduced Fermi energy $\eta$ as argument, and $U_T$ is the temperature voltage.

## III. Results

Fig. 1 shows a comparison of the point wise calculated solution of (7) for different values of $K$ with the polynomial dispersion relation (dashed lines) and the nonparabolic expression (11) (solid lines). The excellent agreement in Fig. 1 justifies to use (11) along with the masses and nonparabolicity coefficients defined in (12) for the characterization of the dispersion relation instead of the polynomial representation.

In Fig. 2 and Fig. 3 we have drawn the parameters defined for the characterization of the subband dispersion relation for different values of the bulk nonparabolicity to see its influence. For usual values for the electric field at the interface - for the presented data the value is approximately 120kV/cm - the variation of the subband nonparabolicity coefficient compared to that of the bulk is

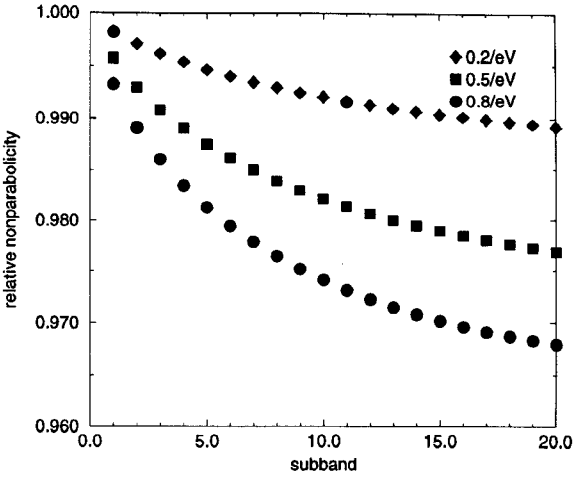


Fig. 2. Relative subband nonparabolicity $\alpha_n/\alpha$ for different values of the bulk nonparabolicity coefficient.

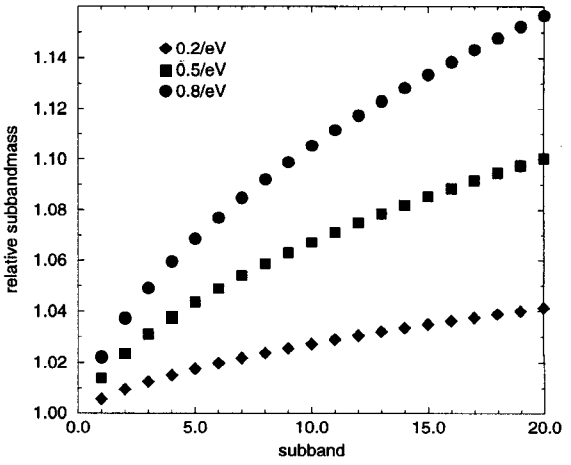


Fig. 3. Relative subband mass $m_n/m$ for different values of the bulk nonparabolicity coefficient.

weak. For $\alpha = 0.5/eV$ and a subband index less than 20 we can see from Fig. 2 that the nonparabolicity coefficient for each subband differs by only a few percents from its bulk value. The dependence of the mass on the nonparabolicity (Fig. 3) is more pronounced. As a first approach it seems therefore realistic for the characterization of the electrons with a dispersion relation (11) to use the bulk values for nonparabolicity coefficients and consider only the mass variations. In Fig. 4 the Fourier coefficients of the first two wave functions are plotted. This corresponds to a representation of the wave functions in momentum space. $N = 64$ harmonics are used.

Due to nonparabolicity the motion of the carriers normal to the interface is no longer decoupled from the mo-

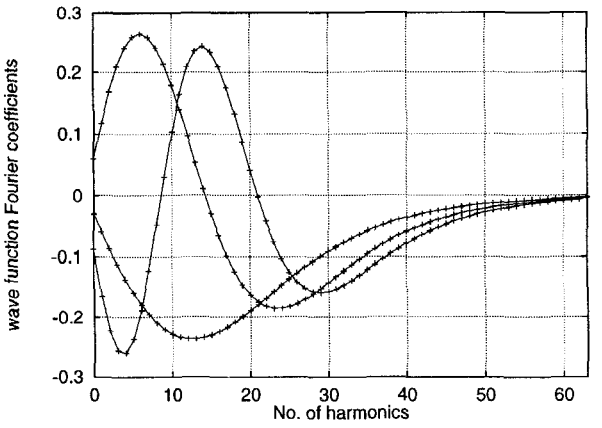


Fig. 4. Spectrum of the first two wave functions.

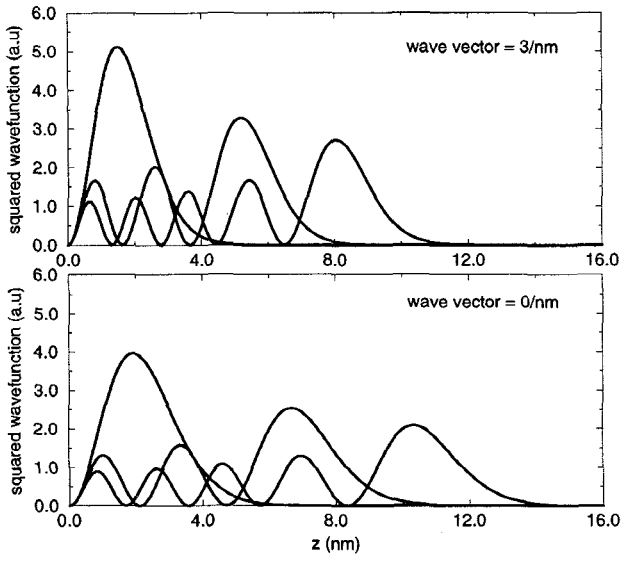


Fig. 5. Squared wavefunction of the first, third and fifth subband for different wave vectors

tion parallel to the interface, as it is the case for parabolic bands. For non-vanishing $K$ narrower wave functions are observed than for $K = 0$ (Fig. 5). This wave function narrowing is more pronounced in higher subbands. Fig. 6 shows the resulting effective widths which are defined as

$$\frac{1}{b_{nn}} = 2 \int |\psi_n(z, K)|^4 dz \,. \tag{20}$$

This parameter is used for the calculation of the scattering rates in a subsequent transport simulation [4]. Seen the variation of the parameters defined in (11) and the dependence of the two-dimensional density of states on the energy, the inclusion of nonparabolicity will lead to higher scattering rates for the nonparabolic case.

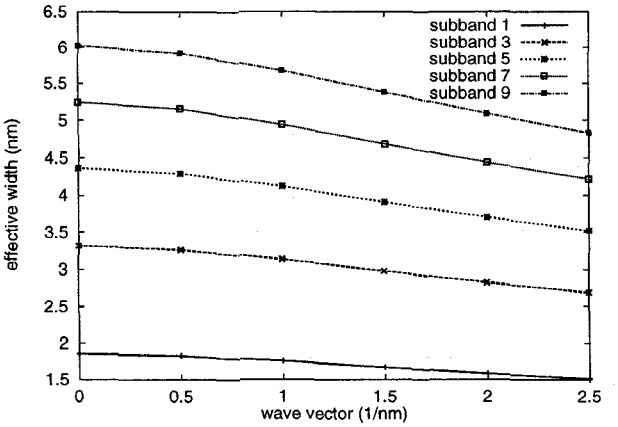


Fig. 6. effective width for different subbands and different wave vectors

## IV. Conclusion

The presented formalism can be considered as a step to a more accurate model for the scattering rates and subsequent transport calculations. Compared to other approaches a consistent nonparabolic subband dispersion relation has been proposed, that will avoid the problems of a polynomial representation. With the described method it is possible to study additional effects introduced by a non-constant subband density of states and wave function narrowing.

## Acknowledgment

This work has been supported by the "Fonds zur Förderung der wissenschaftlichen Forschung", project No: *P10642 PHY.*

## References

[1] Abou-Elnour, A., and Schuenemann, K. A Comparison between Different Numerical Methods Used to Solve Poisson's and Schroedinger's Equations in Semiconductor Heterostructures. *J.Appl.Phys. 74*, 5 (1993), 3273–3276.

[2] Fischetti, M.V., and Laux, S.E. Monte Carlo Study of Electron Transport in Silicon Inversion Layers. *Physical Review B 48*, 4 (1993), 2244–2274.

[3] Jungemann, C., Emunds, A., and Engl, W.L. Simulation of Linear and Nonlinear Electron Transport in Homogeneous Silicon Inversion Layers. *Solid-State Electron. 36*, 11 (1993), 1529–1540.

[4] Yokoyama, K., and Hess, K. Intersubband Phonon Overlap Integrals for AlGaAs/GaAs Single-Well Heterostructures. *Physical Review B 31*, 10 (1985), 6872–6874.